Biogeosciences Discuss., 6, 7481–7515, 2009
www.biogeosciences-discuss.net/6/7481/2009/

Biogeosciences Discussions

Biogeosciences Discussions is the access reviewed discussion forum of *Biogeosciences*

Natural iron enrichment around the Antarctic Peninsula in the Southern Ocean

M. V. Ardelan[1,6], O. Holm-Hansen[2], C. D. Hewes[2], C. S. Reiss[3], N. S. Silva[4], H. Dulaiova[5], E. Steinnes[6], and E. Sakshaug[1]

[1]Norwegian University of Science and Technology (NTNU), Department of Biology, Trondheim, 7491, Norway
[2]Polar Research Program, Marine Biology Research Division, Scripps Institution of Oceanography, University of California-San Diego, La Jolla, Ca 92093-0202, USA
[3]NOAA Fisheries, Antarctic Ecosystem Research Division, La Jolla, CA 92037, USA
[4]Pontificia Universidad Católica de Valparaíso, Escuela de Ciencias del Mar, Chile
[5]Woods Hole Oceanographic Institution, Department of Marine Chemistry and Geochemistry, Woods Hole, MA 02543, USA
[6]Norwegian University of Science and Technology, Department of Chemistry, Trondheim, 7491, Norway

Received: 21 May 2009 – Accepted: 16 June 2009 – Published: 24 July 2009

Correspondence to: M. V. Ardelan (murato@nt.ntnu.no)

Published by Copernicus Publications on behalf of the European Geosciences Union.

Abstract

As part of the US-AMLR program that occupied 99 hydrographic stations in the South Shetland Islands-Antarctic Peninsula region in January–February of 2006, concentrations of dissolved iron (DFe) and total acid-leachable iron (TaLFe) were measured in the upper 150 m at 16 stations (both coastal and pelagic waters). The concentrations in the upper mixed layer (UML) of DFe and TaLFe were relatively high in Weddell Sea Shelf Waters (~0.6 nM and 15 nM, respectively) and lowest in Drake Passage waters (~0.2 nM and 0.9 nM, respectively). In the Bransfield Strait, representing a mixture of waters from the Weddell Sea and the Antarctic Circumpolar Current (ACC), concentrations of DFe were ~0.4 nM and of TaLFe ~1.7 nM. The highest concentrations of DFe and TaLFe in the UML were found at shallow coastal stations close to Livingston Island (~1.6 nM and 100 nM, respectively). The ratio of TaLFe:DFe varied with the distance to land: ~45 at the shallow coastal stations, ~15 in the high-salinity waters of Bransfield Strait, and ~4 in ACC waters. Concentrations of DFe increased slightly with depth in the water column, while that of TaLFe did not show any consistent trend with depth. Our data are consistent with the hypothesis that the relatively high rates of primary production known from the central regions of the Scotia Sea are partially sustained by natural iron enrichment resulting from a northeasterly flow of iron-rich coastal waters originating in the South Shetland Islands-Antarctic Peninsula region.

1 Introduction

Pelagic waters of the Southern Ocean are known for their low chlorophyll-*a* concentration (chl-*a*) albeit some regions, such as the Kerguelen Plateau, Ross Sea, and Scotia Sea significantly elevated concentrations (Sullivan et al., 1993; Holm-Hansen et al., 2004). There are ample evidences that the low chl-*a* concentration in the pelagic part of the Southern Ocean is the result of biomass limiting concentrations of iron (Martin et al., 1990; Boyd and Law, 2001; Öztürk et al., 2004; Hopkinson et al., 2007; Boyd et

al., 2007). Conversely, elevated chl-*a* concentrations in coastal and plateau areas are thought be the result of re-suspension of iron-rich sediments and subsequent upwelling (Korb et al., 2008; Blain et al., 2008; Planquette et al., 2007).

De Baar et al. (1995) have attributed the chl-*a* rich waters in the polar frontal region at ~6° W to upwelling of iron-enriched upper circumpolar deep water resulting from the dynamic polar jet. Much of the Scotia Sea, however, is deep and is distant from the North and South Scotia Ridges as well as the shelf surrounding South Georgia and the South Sandwich Islands. Yet chl-*a* concentration is relatively high (>1.0 mg m^{-3}; Fig. 1a). It is well known that iron originating from sediments on continental shelves enhances productivity in many coastal and shallow water areas (Blain et al., 2007; Pollard et al., 2007; Planquette et al., 2007; Hewes et al., 2009).

One possibility for iron enrichment of the central Scotia Sea is transport from the shelves around the South Shetland Islands (SSI) and the Antarctic Peninsula (Hoppema et al., 2003). Waters from these areas flow in a northeasterly direction toward South Georgia (Hofmann et al., 1996, 1998).

Previous studies (Hopkinson et al., 2007; Hewes et al., 2008) have shown that concentrations of dissolved iron (DFe) around the South Shetland Islands area are high (>1 nM; Fig. 1b), in contrast to the low concentrations in the Antarctic Circumpolar Current (ACC) (<0.50 nM) (Martin et al., 1990; Löscher et al., 1997; Hewes et al., 2008). If enrichment by iron is the major factor promoting the high chl-*a* concentrations in the central Scotia Sea, it is important to determine iron concentrations in the source waters that flow into this region.

The South Shetland Islands-Antarctic Peninsula region is one of the sites where landmasses strongly interacted with Antarctic currents. Therefore US-AMLR studies in this zone provide an opportunity to conduct iron study for a better understanding the effectives of the natural iron enrichment processes and its pathways around SSI-Antarctic Peninsula region. In this paper we provide data on concentrations of both dissolved and total acid-leachable iron (TaLFe) at 16 stations located in both coastal and offshore regions off the South Shetland Islands. These data are discussed in

regard to phytoplankton iron requirements, ratios of dissolved to particulate iron, and the potential importance of natural fertilization with iron from the northern Antarctic Peninsula region for the productivity of the Scotia Sea.

2 Materials and methods

2.1 Field sampling

Water samples were collected during the Antarctic Marine Living Resources program (AMLR) on R/V Yuzhmorgeologiya during the period from 16 January to 8 February 2006 around the Antarctic Peninsula and the South Shetland Islands (Fig. 1). The sampling program included 99 routine CTD (Conductivity-Temperature-Depth) casts to 750 m depth (or to within 10 m of the bottom at shallow stations). Collection of water samples for determination of iron concentrations is described in Sect. 2.1.2.

2.1.1 Routine oceanographic measurements

The CTD sensors were mounted on a carousel unit which also included a Chelsea profiling fluorometer for measuring in situ chl-*a* fluorescence, a Wet Labs profiling transmissometer for measuring light attenuation at 660 nm, and ten 8-liter General Oceanics Niskin bottles. Continuous profiles were obtained on the down casts. Water samples for chl-*a* and macronutrient determinations were obtained from the Niskin bottles during up casts at 200, 100, 75, 50, 40, 30, 20, 15, 10, and 5 m depths.

2.2 Chlorophyll-*a* determination

Chl-*a* concentrations (mg m^{-3}) were determined fluorometrically. Sample volumes of 100 ml were filtered through glass fiber filters (Whatman GFF, 25 mm) at a differential pressure of <1/3 atmosphere. The filters with the particulate material were placed in 10 ml of absolute methanol in 15-ml tubes and the photosynthetic pigments extracted

at 4°C for at least 12 h. The samples were then shaken and centrifuged, and the clear supernatant poured into cuvettes (13×100 mm) for measurement of chl-*a* fluorescence before and after the addition of 2 drops of 1.0 HCl (Holm-Hansen and Riemann, 1978). Fluorescence was measured using a Turner Designs model 700 fluorometer that had been calibrated using a prepared chl-*a* standard (Sigma C-6144) and also with the concentration determined by optical density measurements. Stability of the fluorometer was verified daily by use of a solid-state fluorescence standard (Turner Designs No. 7000-994).

2.3 Macronutrient determination

Water samples (∼50 ml) for analysis of macronutrients were poured from the Niskin bottles into acid-cleaned (1 N HCl) polyethylene bottles of 60 ml volume. The samples were subsequently maintained at −20°C until analysis. An autoanalyzer was used for determination of nitrate + nitrite, phosphate, and silicic acid (Atlas et al., 1971). We here use the term nitrate for the sum of nitrate and nitrite.

2.4 Upper mixed layer depth determination

Depth of the upper mixed layer (UML) was calculated as the depth at which potential density (σ_θ) differed by 0.05 from the mean potential density measured between 5 and 10 m depth.

2.5 DFe and TaLFe sampling and determination

Water samples were collected with acid-cleaned Teflon-lined GO-FLO bottles deployed on trace metal clean polymer 1/4″ Sta-Set X linen (New England ropes) line using a dedicated winch. The samples were taken from depths ranging from 10 to 175 m to represent the upper mixed layer (UML) and water below the pycnocline. The bottles were taken to a clean room, placed on a rack under clean air blowing from a Class-100 laminar flow hood. Processing of the samples started immediately. The samples

were first collected in acid-cleaned, 0.5 and 1.0 liter low-density polyethylene (Nalgene) bottles, from which the water DFe analysis was pumped through acid-washed Tygon tubes by a peristaltic-pump throught acid-washed Sartobran-Sartorious filters (0.4 μm pore size pre-filteation followed by a 0.2 μm pore size filtration). The DFe fractions were thus defined operationally by the 0.2 μm nominal pore size and therefore include colloidal Fe. During filtration an additional HEPA air-filter cartridge (HEPA-CAP/HEPA VENT, 75 mm, Whatman) was connected to the pressure-relief/air-vent valve of the GO-FLO bottles in order to ensure that the air in contact with the sample during the filtration was clean. Water samples for TaLFe determination were pumped directly into the polyethylene bottles without filtration. All samples for DFe and TalFe were acidified to pH 1.7–1.8 with 15.4 M ultrapure HNO_3 (optima grade, Sigma). The acidified water samples were returned to NTNU and stored for about 7–8 months before analysis.

Pre-concentration of DFe and TaLFe from seawater was carried out by a modified combination of Chelex-100 (Na^+ form, 100–200 mesh size, Bio-Rad) batch (Baffi and Cardinale, 1990; Grotti et al., 2001) and column technique (Öztürk, 1995; Öztürk et al., 2002).

Before the Chelex treatment, ∼500 ml of the acidified samples were microwaved for 2.5 min at ∼60°C, allowed to cool for 30 min, and then microwaved again for 2.5 min. This breaks down the remaining strong ligand-Fe complexes and colloidal iron. The procedure is necessary to convert the strong ligand-iron complexes that might not be labile in Chelex-100 into labile forms (Bruland and Rue, 2001; Bruland et al., 2005). The pH of the acidified and microwaved samples was brought to 5.7–5.9 by addition of 1.6 M ultra-pure ammonium acetate buffer immediately before addition of the Chelex-100 slurry, (prepared as described below).

Chelex-100 resin was carefully cleaned by repetitive washes with 3 M ultra-pure HCl (isothermally distilled), 2 M ultra-pure HNO_3 (optima grade, Sigma), and Milli-Q water (18.4 mΩ) and then converted to NH_4^+ by using isothermally distilled NH_4OH (see Öztürk et al., 2002, for details of preparation and cleaning the Chelex-100). An aliquot of 0.8 ml) of the Chelex-100 slurry (0.35–0.45 g dry weight of resin) was added to 500 ml

of seawater that had been buffered to pH 5.7–5.9, which is the optimal pH range for iron pre-concentration on Chelex-100. The samples with Chelex-100 were shaken at 70 rpm for 48 h at room temperature. All sample treatments and pre-concentration were done in a Class-100 clean laboratory at the Dept of Chemistry at NTNU.

The samples with Chelex-100 were transferred to an acid-cleaned plastic Bio-Rad column system pre-loaded with ∼0.1 g clean Chelex-100 resin and allowed to run at a rate of ∼2 ml min^{-1}. When this step was completed, the Chelex-100 in the column was washed with 20 ml of Milli-Q water and 10 ml 0.1 M ultra-pure ammonium acetate buffer solution to remove the residue of seawater matrix. For extraction of iron from Chelex-100, 1.0 ml of 2 M ultra-pure HNO_3 was added to the column and allowed to react for 10 min, after which the column was gently shaken in order to maximize the contact beween the Chelex-100 resin and the HNO_3, after which 1.0 ml of the HNO_3 extract in the column was carefully transferred into an acid-washed 10 ml PE tube. The same procedure was repeated with 4 ml of 0.25 M ultra-pure HNO_3. After 30 minutes, this extract was added to the PE tube containing the first extract. The final volume, 5.0 ml represents a pre-concentration factor of 100.

DFe and TaLFe were measured using a High Resolution Inductive Coupled Plasma Mass Spectrometer (HR-ICP-MS) Element 2 (Thermo-Finnigan) with PFA-Schott type spray chamber and nebulizer. Plasma and mass spectrometer parameters were optimized daily at a medium resolution of 4000. Mass window was 100%. The nebulizer gas flow optimization was done daily. 0.6 M ultra-pure HNO_3 was used for flushing the sampler prop and sample loop The sample uptake rate to plasma was 0.25 mL min^{-1} with a sample/peak ratio of 20. Each analysis used 0.8 ml sample and 1.2 ml washing acid. As the washing and sample scanning times took 30 s, the total time required for three scans of each sample was 90 s. In order to lower the instrumental Fe blank values, 0.6 M ultra-pure HNO_3 was run before sample measurements. Element 2 software was used for the analysis.

2.6 Calibration and performance of iron determination

Accuracy and precision of the iron determination method were checked using the certified standard materials NASS-5 (National Research Council of Canada). Recovery tests were also carried out with seawater spiked with various Fe enrichments, and showed good recovery (accuracy and precision are summarized in Table 1).

The data reported in this paper represent total concentrations of dissolved iron and the acid-leachable (pH≤1.8) fraction of the total iron. Thus, the data do not include iron from iron-containing particulate material, which is acid-refractory. From an ecological point of view this is not a serious because iron in acid-refractory particles is most likely not available to microbial cells. Comparison between spiked seawater samples and microwaved NASS 5 revealed that microwaving of the acidified samples managed to quantitatively liberate the Fe from iron-organic complexes stronger than those between iron and the iminodiacetic acid functional group of Chelex-100; thus, indicating that DFe was quantitatively pre-concentrated by Chelex-100.

3 Results

3.1 Iron concentrations in the upper water column

Data for the 16 stations shown in Fig. 1b have been divided into five groups (A–E, Table 2). The waters in the southern portion of Bransfield Strait (group A, stations 1–4) were coldest, had the highest salinity, and had relatively low chl-*a* concentrations. Group B (stations 5–7), represents the deep waters of Bransfield Strait close to the shelf break and also exhibited high chl-*a* concentrations of (>1.0 mg m^{-3}). Group D (stations 10–13) represents the deep offshore stations with waters that are characterized by the highest surface temperatures, lowest salinity, and lowest chl-*a* concentrations. Highest chl-*a* concentrations were recorded at the three inshore stations 14–16 that form group E and the two inshore stations 8 and 9 in deep water very close to the

shelf break (group C). The t/s diagrams for the 16 stations (Fig. 2), show that stations within each of the five groups are quite similar and that each group is quite distinct from the other four.

When the iron concentrations from all sampling depths at the 16 stations are plotted against density, it can be seen that the highest concentrations of both DFe and TaLFe are found in waters with high the highest σ_θ, and that the lowest Fe concentrations are found in low-density waters of Drake Passage (Fig. 3). The stations with the highest concentrations of DFe and TaLFe were the near-shore stations 14–16 (group E), which differed in terms of the iron concentration vs. water density from tbe other stations (enclosed by circles in Fig. 3a and b). With exception of the inshore data, the TaLFe/DFe ratio varied from ∼4 in low salinity waters to ∼15 in high salinity waters. The ratio for the three inshore stations (group E) ranged from ∼12 to 63, with a mean of 45.

Profiles of DFe and TaLFe concentrations vs. depth (0–200 m) for all stations in each group (Fig. 4), and corresponding profiles of water density (0–400 m) show that DFe concentrations were lowest in or slightly below UML, with concentrations increasing at greater depths whereas data for TaLFe did not display any consistent pattern.

When the averages for temperature, chl-*a*, nitrate, phosphate, DFe, and TaLFe in the UML at the 16 stations are plotted against salinity (Fig. 5), the data for individual stations within each group (Table 2) are fairly close with each group distinct from the other groups. The stations in group A (southern part of the Bransfield Strait) exhibited the lowest temperature (Fig. 5a), low chl-*a* values (Fig. 5b), and highest nitrate and phosphate concentrations (Fig. 5c and d) and highest DFe and TaLFe concentrations (except for the three shallow stations of group E; Fig. 5e and f). The Drake Passage (Group D) exhibited the highest temperature and the lowest concentrations of chl-*a*, macro nutrient, DFe, and TaLFe. Again group E was different, with the highest concentrations of both DFe (>1.0 nM) and TaLFe (>2.0 nM) in combination with high chl-*a* concentration (>2.0 mg m^{-3}). Chl-*a* concentrations exhibited a unimodal relationship with salinity with the maximum concentrations at S∼34 (Fig. 5b).

Judging from the data in Figs. 3 and 5, shallow-water group E stations had the highest DFe and TaLFe concentrations in combination with low salinity (∼34.1) as compared to the average salinity of ∼34.3 for stations A. It is likely that the high Fe concentrations were associated with release of Fe from re-suspending bottom sediments or runoff from the land. Evidence for re-suspension could be seen from profiles of in situ chl-*a* fluorescence and light attenuation at the six stations in the coastal survey (Fig. 6). The six stations were characterized by high in situ chl-*a* fluorescence in the upper 50 m and indetectable in situ chl-*a* fluorescence >200 m depth. The transmissometer data, however, showed that at the three outermost among the group E stations the beam attenuation decreased rapidly from 50–100 m depth, remained low from 100–200 m depth, and was very low and ∼constant down to 350 m depth. In contrast, the beam attenuation at the three stations close to the shore was high from 100–350 m depth. As the high attenuation of light cannot be attributed to absorption by chl-*a*, it is likely to have been caused re-suspended particulate material from the bottom sediments.

3.2 Co-variation between DFe and TaLFe concentrations

Concentrations of TaLFe, which belongs to in the particulate fraction increased more rapidly than concentrations of DFe with increasing density (Fig. 3 and 7). Concentrations of DFe seemed to level off at ∼2.5 nM. The ratio of TaLFe/DFe decreased from ∼60 in shallow waters (90 m) close to shore to ∼9.4 in deep water (1200 m) 50 km from the shore (Fig. 8).

3.3 Co-variation between Fe and macro-nutrients

Concentrations of DFe and nitrate (Fig. 9a) and phosphate (Fig. 9b) covaried. The change in concentrations of nitrate and phosphate relative to that of DFe, however, differed between the Bransfield Strait (dark symbols in Fig. 9) where concentrations of DFe are relatively high as compared to the off shore stations (open symbols in Fig. 9) where DFe concentrations are generally low.

4 Discussion

4.1 Fe concentrations: association with hydrography and surface transports

In order to understand the distribution of iron based on the 16 stations, it is important to know the general circulation for surface waters in the AMLR survey area. The flow pattern of surface is complicated, as illustrated by Lagrangian drifter tracks (Fig. 10a). Bottom topography, such as the Shackleton Transverse Ridge and the continental shelf break strongly influence the flow .The drifters were often concentrated in fast moving jets, such as the drifter flowing in a northeasterly direction along the shelf break to the south of the South Shetland Islands, and the jet flowing in a northwesterly direction between the Powell Basin and Joinville island. The drifter tracks in Bransfield Strait (black) shows eddies to the south of King George Island (with the center of an eddy over deep water in the central basin, and close to the location of station 7), a smaller eddy at ∼55.5° W, and a larger one over shallow water close to 54° W (center located close to the station 1). Evidently the surface waters in Bransfield Strait originate primarily from the Powell Basin region of the Weddell Sea (Fig. 10b). This outflow from the cyclonic Weddell Sea gyre becomes enriched by sediment-derived Fe while passing the shallow shelf regions of the Weddell Sea and the Antarctic Peninsula before trifurcating, with one part flowing toward the southwest over the northern shelf regions of the Antarctic Peninsula. Another part flows to the northwest in the direction of Elephant Island,,forming an anti-cyclonic eddy in Bransfield Strait, and the third part flows northwards and then northeast. In the southern region of Bransfield Strait the Fe-enriched cold, high salinity waters from the Weddell Sea mix with the warmer and fresher waters originating from the Drake Passage and the Bellingshausen Sea and flows to the northeast (Zhou et al., 2006).

The iron data (Fig. 5e and f) show that (i) the highest iron concentrations occurred at the shallow, near-shore stations 14–16, and that (ii) the next highest concentrations were in the Bransfield Strait (stations 1–4), followed by stations 5–9, where Fe concentrations were still fairly high, and that (iii) the lowest Fe concentrations were in deep

Drake Passage waters (stations 10–13). This is consistent with the flow pattern in the investigated area (Fig. 10b) indicating that iron-rich waters originate in the Weddell Sea (Westerland and Öhman, 1991; Sañudo-Wilhelmy et al., 2002) and subsequently mix with iron-poor waters from the Drake Passage (Hewes et al., 2008, 2009). DFe concentrations in the Weddell Sea ranged from 0.24–5.6 nM (Westerlund and Öhman, 1991), in the region of the Weddell-Scotia Confluence ∼4–8 nM (de Baar and de Jong, 2001), and 50 nM in shallow, near-shore waters (de Baar and de Jong, 2001 and references therein). Similarly, Martin et al. (1990) reported 0.16 nM Fe in Drake Passage waters and 7.4 nM Fe in neritic Gerlache Strait waters. Our DFe data for the Bransfield Strait and the coastal zones are lower, probably because of consumption by phytoplankton, which had attained exceptionally high biomass during our cruise compared to previous years (Hewes et al., 2009). On the other hand, our DFe data were comparable with those reported by Sañudo-Wilhelmy et al. (2002) that ranged from 0.5–2.2 nM near the western rim of the Weddell Sea, and 4.5–30 nM at near-shore stations. Hewes et al. (2008) reported DFe concentrations for the UML from ∼0.3 nM in the ACC to ∼2.0 nM in Bransfield Strait.

TaLFe-rich waters in the near-shore and shallow zones and relatively high concentrations in the Bransfield Strait indicate that much of the TaLFe in the particulate fraction originates from coastal sediments. Concentrations of DFe had an upper limit of ∼2.5 nM (Fig. 7), despite the increasing concentrations of TaLFe. Upper limits of DFe in seawater are chemically controlled by the solubility of iron particles, including adsorption/desorption of DFe onto particles, the complexation of iron with strong and weak organic ligands (Boye et al., 2005; Croot et al., 2004), formation of organic and inorganic iron-colloids and involvement of other biological processes (Barbeau et al., 1996; Tovar-Sanchez et al., 2007; Sato et al., 2007; Frew et al., 2006; Pollard et al., 2007). The concentrations of DFe in our study are positively correlated with the concentration of TaLFe (Fig. 7), but when waters are transported offshore, much of the TaLFe apparently settles out of the euphotic zone faster than the DFe fraction. The ratio of TaLFe/DFe thus varies with the distance from the shore and the depth of the

water column.

The mean TaLFe/DFe ratio at the near-shore stations 14–16 was ~60 (mean water depth 446 m); at stations 1–4 in the southern portions of Bransfield Strait the mean ratio was 21 (mean depth 389 m), while at the deep Stations 5–13 the mean ratio was 4.3 (mean water depth 2563 m). With only TaLFe and DFe data available it is impossible to understand the details of the mechanisms that control the upper limits of the dissolved Fe. However, the logarithmic correlations between TaLFe and DFe (DFe=0.31*Ln(TaLFe)+0.34, r2=0.78 for all data, and DFe=0.45*Ln(TaLFe)+0.01, r2=0.84 for coastal survey area) in our data imply that when the particle input is high, loss of DFe due to abiotic particle scavenging might be more effective than the release of dissolved iron from re-suspended particles. In fact, there are indirect indications of intense near-shore removal processes of dissolved iron (Bucciarelli et al., 2001).

4.2 Scale lengths of Fe transport

Possibly soluble/bioavailable iron can be leached from suspended TaLFe fractions of particulate Fe during lateral onshore-offshore transport. The relatively high concentrations of TaLFe in the surface waters of the northern section of the Bransfield Strait indicate that transport of particulate iron from both sediment and coastal systems is effective. During this transport lithogenic iron is transformed into biogenic iron in the euphotic zone, after which it re-solubilizes below the euphotic zone where it is effectively scavenged by settling particles (Frew et al., 2006). The length scale of iron transport from a coastal system to the open ocean also depends on the currents in the particular area. Iron transport could be effective in a downstream current from a shallow coastal system to the open ocean (e.g., the northeasterly flow of coastal waters out of Bransfield Strait into the Scotia Sea). In contrast, when the main current flows parallel to the shelf, export from the coastal system into the open ocean would be less effective. Previous studies in our sampling area also demonstrate that lateral transport in transects from the coast to Drake Passage (perpendicular to the main currents) was not as efficient as that in the Bransfield Strait-Elephant Island sections (Dulaiova et

al., 2009). To estimate how effective the coastal inputs are for long-range bio-available iron transport, including northward transport by the slower meridional flow (Cassar et al., 2008), we calculated "scale length" of the DFe and TaLFe concentrations from the coastal survey data in two transects which were perpendicular to the coastal currents to the northwest of Livingston Island (Figs. 1b and 10b). We used scale length (SL) in this context as "the distance over which concentrations drop to 1/e (=0.37) of the initial Fe concentration" at the shore (Johnson et al., 1997). We estimated SL for DFe (SL_{DFe}) and TaLFe (SL_{TaLFe}) by plotting DFe and TaLFe from coastal survey stations vs. distance from shoreline (Fig. 8). Surface data (<50 m depth) fit by exponential regressions, indicates SL_{DFe} and SL_{TaLF} of 25 and 12 km, respectively. These lengths indicate that neither dissolved nor particulate iron penetrate far into open ocean in the latitudinal/meridional direction when the main current is parallel to the coast. Our estimate of SL_{DFe} of 25 km is identical to the SL_{DFe} found by Planquette et al. (2007) and is comparable to the SL_{DFe} (16 km) found by Johnson et al. (1997) for Monterey Bay. However, SL_{DFe} estimated for near-shore waters off Kerguelen Islands was 151 km (Bucciarelli et al., 2001) and for waters near the Galapagos Islands, 103 km (Gordon et al., 1998). The differences were attributed to different water circulation patterns in those coastal systems and the difference between the respective surface areas of the islands (Planquette et al., 2007). Geochemical characteristic of the source area, type of continental shelf and margin and, differences in biological processes might also play a role.

4.3 Cellular quotas of iron and carbon, and estimation of iron supply

Bio-available Fe input into the Antarctic Peninsula-Bransfield Strait region supports high rates of primary production in the South Shetlands Islands area as well as in the western Scotia Sea. It is therefore relevant to obtain an idea of the mean cellular iron quota (Fe:C) for the phytoplankton community and to compare with other regions. Crude estimates of cellular iron quota can be obtained by proxy from Redfield ratios (Sunda and Huntsman, 1995), assuming that the slopes of regressions of iron vs. phos-

phate concentrations with depth provide an indicator of cellular Fe:P ratios. Similarly we assume that concentrations in the pycnocline represent winter surface values, and derived drawdown ratios for Fe and NO_3, such that

$$\Delta Fe/\Delta NO_3 = (DFe_{pycnocline} - DFe_{UML})/(NO_{3\,pycnocline} - NO_{3\,UML}), \quad (1)$$

where $DFe_{pycnocline}$, $NO_{3\,pycnocline}$ are mean concentrations at the pycnocline, and DFe_{UML} and $NO_{3\,UML}$ are mean concentrations of the UML. For the pycnocline, mean DFe, and NO_3 concentrations were ∼1 nM and 30.5 μM, respectively, and for the UML, DFe and NO_3 were ∼0.5 nM and ∼27 μM, respectively. For Bransfield Strait, $\Delta Fe{:}\Delta NO_3$=0.17 nmol:μmol being the same as the slope of the regression between DFe and NO_3 for all data (Fig. 9a). Similarly, $\Delta Fe{:}\Delta NO_3$=0.05 nmol:μmol for Drake Passage, also close to the slope of 0.04 from regression between DFe and NO_3 for all data (Fig. 9a). Redfield ratios provide Fe:C=6±3 μmol:mol in the Drake Passage water and 26±7 μmol:mol in Bransfield Strait when C:N=6.6 mol:mol. Similarly, from the slope of DFe vs. P (Fig. 9b) we estimate Fe:C=5.2±3 and 17.2±4 μmol:mol in the Drake Passage and Bransfield Strait, respectively, when C:P=106 mol:mol. Such estimates do not take into account different flow and dilution rates of isopycnals that move up and down in (Hewes et al., 2008). This would lead to different residence times of Fe, P, and N in both the UML and pycnocline, as well as, different regeneration rates of Fe and macronutrient through grazing processes (Frew et al., 2006). However, such values are comparable with those obtained from the Southern Ocean Iron Experiment (SOFeX) for Fe:C of ∼10 μmol:mol under Fe-stress and ∼40 μmol:mol with Fe-enrichment (Twining et al., 2004). Variation in published cellular Fe:C ratio is large depending on the method used to obtained it and the location (Boyd et al., 2007 and reference therein). In the Southern Ocean, the published Fe:C ratio varies from ∼5 to ∼50 μmol:mol and can increase ≥100 μmol:mol in artificial Fe enrichment experiments (Boyd et al., 2007).

The iron demand of phytoplankton can be estimated from Fe:C and primary productivity. Total primary production can be estimated (Holm-Hansen and Mitchell, 1991) as:

mg carbon fixed $m^{-2}\,d^{-1}$=0.32* (mg Chl-*a* m^{-2})* (Einstein $m^{-2}\,day^{-1}$)

with Chl-*a* integrated through the euphotic zone. Mean incident PAR during the 2006 survey was obtained from direct measurements of cosine PAR taken aboard ship, with daylight (08:00–24:00 GMT) hours only considered (38.1 Einstein $m^{-2}\,d^{-1}$), and euphotic zone estimated directly from daytime stations. Mean rates of daily primary production for DrakePassage and Bransfield Strait were estimated at 278 mg C $m^{-2}\,d^{-1}$ (mean euphotic depth 54 m) and 600 mg C $m^{-2}\,d^{-1}$ (mean euphotic depth 35 m), respectively. Despite the fact that this estimation of primary production may have some degree of uncertainty, it is still useful to make estimation for the range of the iron demand in the region. Total primary productivity was factored by 0.15 (Drake Passage) and 0.22 (Bransfield Strait) to obtain amounts of "new" primary production (factor values based on rates of nutrient regeneration where the f-values averaged ∼0.15 in Drake passage stations and 0.22 in Bransfield straits as reported by Rönner et al. (1983) and Koike et al. (1986). Hence, mean daily rates of new primary production at the Drake Passage and Bransfield stations would be 42 and 132 mg C $m^{-2}\,d^{-1}$ (3.5 and 11 mmol C $m^{-2}\,d^{-1}$), respectively.

The integrated Fe demand can be calculated by using Eq. (2)

$$Fe_{demand} = newPP \times (Fe : C)_{cellular} \quad (2)$$

and cellular Fe:C estimated to be ∼ 6 and ∼26 μmol mol^{-1} for Drake passage and Bransfield Strait zones, respectively.

For the euphotic zone in Drake passage and Bransfield Strait stations, a rough estimate of integrated Fe demand would thus be ∼21 and ∼286 nmol $m^{-2}\,d^{-1}$, respectively. The Fe demand in Bransfield Strait is apparently >10 times higher than that in the Drake Passage.

Calculated lateral DFe supply based on Fe/^{228}Ra ratios in the Elephant Island zone (the northeast region of Bransfield Strait) was around 1800 nmol $m^{-2}\,d^{-1}$ (Dulaliova et al., 2009). This lateral Iron supply is beyond the estimated integrated Fe demand of ∼286 nmol $m^{-2}\,d^{-1}$ in Bransfield Strait. This estimation indicates that lateral supply of

DFe should be more than enough to support the observed primary productivity in the northeast region of Bransfield Strait.

4.4 Sources of Fe to support high phytoplankton biomass in the Scotia Sea

Satellite imagery shows that both Drake Passage and Weddell Sea waters have very low chl-*a* concentrations during the austral summer, in contrast to the high chl-*a* concentrations over the northern and southern continental shelf regions of the South Shetland Islands, including Elephant Island (Fig. 1). Phytoplankton biomass are known to be Fe-limited in Drake Passage waters (Martin et al., 1990; Helbling et al., 1991; Hopkinson et al., 2007). In contrast, deep surface mixing (not Fe) probably limits phytoplankton biomass in high salinity Weddell water (Hewes et al., 2008; see Fig. 5b). High chl-*a* concentrations (>1.0 mg m^{-3}) around the South Shetland Islands spread as a band toward the northeast over the deep waters of the central Scotia Sea (Fig. 1a) and stretches all the way to ∼40° W, to the southwest of South Georgia. Much of this chl-*a* rich region in the Scotia Sea lies in ACC waters to the north of the Southern Extent of Antarctic Circumpolar Current sequence waters (SEACC), with the rest lying in the mixing zone between the SEACC and the Northern Extent of Weddell Sea sequence waters (Whitworth et al., 1994). Since no Fe data is available for this region, the high phytoplankton biomass in the central Scotia Sea can only be speculated upon yet is presumably the result of natural Fe fertilization from the peninsular area.

The major sources of waters in the Scotia Sea are (i) ACC waters flowing through Drake Passage, (ii) waters from Bransfield Strait and the shelf regions of the SSI, and (iii) Weddell Sea waters flowing directly into the Scotia Sea. Surface waters of the ACC just to the west of Drake Passage have low concentrations of both DFe (<0.2 nM) and TaLFe (<0.50 nM) as reported by de Baar and de Jong (2001). These concentrations are slightly lower than we found in the ACC waters (see Fig. 5e and f), and the concentrations are not capable of supporting high chl-*a* concentrations (Martin et al., 1990; Helbling et al., 1991; Hopkinson et al., 2007) as observed for the Scotia Sea. In contrast to ACC waters, the waters of Bransfield Strait and the shelf regions of

the SSI (Fig. 5; Sañudo-Wilhelmy et al., 2002; Hewes et al., 2008) have much higher concentrations of both DFe and TaLFe.

The concept that natural phytoplankton assemblages are Fe-limited in ACC waters but not in Bransfield Strait waters is supported by the Fe-addition experiments by Helbling et al. (1991) and Hopkinson et al. (2007). The high chl-*a* regions (Fig. 1a) suggest that the northeasterly flow of Fe-enriched waters from the peninsular region may be responsible for the high chl-*a* concentrations in the central portion of the Scotia Sea. Although the southern regions of the Scotia Sea close to the Scotia Ridge are enriched in Fe from sediments on the the South Scotia Ridge (de Baar et al., 1990), as well as from Fe-rich Weddell Sea waters flowing north through the deep Philip Passage to the west of the South Orkney Islands (Foster and Middleton, 1984), concentrations of chl-*a* indicate that such Fe-enriched waters do not extend very far north into the central Scotia Sea (Biggs et al., 1982). Water from the Scotia Sea also flows north in the deep passages of the Scotia Ridge to the east of the South Orkney Islands (Heywood et al., 2004), but this abyssal flow of Weddell Sea water into the Scotia Sea apparently has no surface expression.

Our results with the circulation patterns provide evidence for natural iron enrichments in the region and allow us to suggest that northeastward horizontal advection from the South Shetland Islands-Antarctic Peninsula coastal system carries necessary iron to support the relatively high rates of primary production known from the central regions of the Scotia Sea

Future studies, however, must consider other possible sources of Fe enrichment in surface waters of the Scotia Sea, which include (i) upwelling associated with the many frontal systems in the Scotia Sea (Löscher et al., 1997; Holm-Hansen et al., 2004), (ii) eddy formation, which involves both downwelling and upwelling (Kahru et al., 2007), (iii) isopycnal mixing south of the Polar Front (Pollard et al., 2006), (iv) upwelling of isopycnals over shallow topographical features (Sullivan et al., 1993; Holm-Hansen et al., 2005), and (iv) aeolian input.

Acknowledgements. We wish to thank the officers and crew of R/V Yuzhmorgeologiya for their invaluable help during the course of this field study. The authors are very grateful to Svein Kristiansen from University of Tromsø, for lending his GO-FLO bottles and S. Lierhagen for his contribution performing the HR-ICP-MS anlysis. This work was supported by the Norwegian Polar Institute (grant 3557-103 – E. Sakshaug) and the US AMLR program, administered by the Antarctic Ecosystem Research Division at NOAA's Southwest Fisheries Research Center, La Jolla, California, under grant NA17RJ1231 (O. Holm-Hansen). Views contained herein are those of the authors and do not reflect those of NOAA.

References

Atlas, E. L., Gordon, L. I., Hager, S. W., and Park, P. K.: A Practical Manual for Use of the Technicon Autoanalyzer in Seawater Nutrient Analyses (Revised), Tech. Report 215, Department of Oceanography, Oregon State University, Corvallis, OR 97331, 1971.

Baffi, F. and Cardinale, A.: Improvements in use of Chelex-100 resin for determination of copper, cadmium and iron in seawater, Int. J. Environ. An. Ch., 41, 15–20, 1990.

Barbeau, K., Moffett, J. W., Caron, D. A., Croot, P. L., and Erdner, D. L.: Role of protozoan grazing in relieving iron limitation of phytoplankton, Nature, 380, 61–64, 1996.

Biggs, D. C., Johnson, M. A., Bidigare, R. R., Guffy, J. D., and Holm-Hansen, O.: Shipboard autoanalyzer studies of nutrient chemistry, 0–200 m, in the eastern Scotia Sea during FIBEX (January–March 1981), Texas A&M University, Department Oceanography Technical Reports, 88-11-T, 1982.

Blain, S., Queguiner, B., Armand, L., et al.: Effect of natural iron fertilization on carbon sequestration in the Southern Ocean, Nature, 446, 1070–1074, 2007.

Blain, S., Sarthou, G., and Laan, P.: Distribution of dissolved iron during the natural iron fertilization experiment KEOPS (Kerguelen Plateau, Southern Ocean), Deep Sea Res. Pt. II, 55, 594–605, 2008.

Boye, M., Nishioka, J., Croot, P. L., Laan, P., Timmermans, K. R., and de Baar, H. J. W.: Major deviations of iron complexation during 22 days of a mesoscale iron enrichment in the open Southern Ocean, Mar. Chem., 96, 257–271, 2005

Boyd, P. W. and Law, C. S.: The Southern Ocean Iron RElease Experiment (SOIREE) – introduction and summary, Deep-Sea Res. Pt. II, 48, 2425–2438, 2001.

Boyd, P. W., Jickells, T., Law, C. S., Blain, S., Boyle, E. A., Buesseler, K. O., Coale, K. H., Cullen, J. J., de Baar, H. J. W., Follows, M., Harvey, M., Lancelot, C., Levasseur, M., Owens, N. P. J., Pollard, R., Rivkin, R. B., Sarmiento, J., Schoemann, V., Smetacek, V., Takeda, S., Tsuda, A., Turner, S., and Watson, A. J.: Mesoscale iron enrichment experiments 1993–2005: synthesis and future directions, Science, 315, 612–617, 2007.

Bruland, K. W. and Rue, E. L.: Iron: analytical methods for the determination of concentrations and speciation, in: The Biogeochemistry of Iron in Seawater, edited by: Hunter, K. A. and Turner, D. R., IUPAC Book Series on Analytical and Physical Chemistry of Environmental Systems, John Wiley and sons, Chichester, UK, 255–289, 2001.

Bruland, K. W., Rue, E. L. Smith G. J., and DiTullio, G. R.: Iron, macronutrients and diatom blooms in the Peru upwelling regime: brown and blue waters of Peru, Mar. Chem., 93, 81–103, 2005.

Bucciarelli, E., Blain, S., and Tréguer, P.: Iron and manganese in the wake of the Kerguelen Islands (Southern Ocean), Mar. Chem., 73, 21–36, 2001.

Cassar, N., Bender, M. L., Barnett, B. A., Fan, S., Moxim, W. J., Levy II, H., and Tilbrook, B.: Response to Comment on "The Southern Ocean Biological Response to Aeolian Iron Deposition", Science, 319(5860), 159b, 2008.

Croot, P. L., Andersson, K., Öztürk, M., and Turner, D. T.: The distribution and speciation of iron along 6° E in the Southern Ocean, Deep-Sea Res. Pt. II, 51, 2857–2879, 2004.

de Baar, H. J. W., de Jong, J. T. M., Bakker, D. C. E., Löscher, B. M., Veth, C., Bathmann, U., and Smetacek, V.: Importance of iron for plankton blooms and carbon dioxide drawdown in the Southern Ocean, Nature, 373, 412–415, 1995.

de Baar, H. J. W., Buma, A. G. J., Nolting, R. F., Cadee, G. C., Jacques, G., and Treguer, P. J.: On iron limitation of the Southern Ocean: experimental observations in the Weddell and Scotia Seas, Mar. Ecol.-Prog. Ser., 65, 105–122, 1990.

de Baar, H. J. W. and de Jong, J. T. M.: Distributions, Sources and Sinks of Iron in Seawater, in: The Biogeochemistry of Iron in Seawater, edited by: Hunter, K. A. and Turner, D. R., IUPAC Book Series on Analytical and Physical Chemistry of Environmental Systems, John Wiley and sons, Chichester, UK, 123–254, 2001.

Dulaiova, H., Ardelan, M. V., Henderson, P. B., and Charette, M. A.: Shelf-derived iron inputs drive biological productivity in the Scotia Sea, Global Biogeochem. Cy., in review, 2009

Foster, T. D. and Middleton, J. H.: The oceanographic structure of the eastern Scotia Sea – I. Physical oceanography, Deep-Sea Res., 31, 529–550, 1984.

Frew, R. D. Hutchins, D. A., Nodder, S., Sanudo-Wilhelmy, S., Tovar-Sanchez, A., Leblanc, K., Hare, C. E., and Boyd, P. W.: Particulate iron dynamics during FeCycle in sub-antarctic waters southeast of New Zealand, Global Biogeochem. Cy., 20, GB1S93, doi:10.1029/2005GB002558, 2006.

Gordon, R. M., Johnson, K. S., and Coale, K. H.: The behavior of iron and other trace elements during the IronEx-I and PlumEx experiments in the Equatorial Pacific, Deep-Sea Res. Pt. II, 45, 995–1041, 1998.

Grotti, M., Soggia, F., Abelmoschi, M., Rivaro, P., Magi, E., and Frache, R.: Temporal distribution of trace metals in Antarctic coastal waters, Mar. Chem., 76, 189–209, 2001.

Helbling, E. W., Villafane, V., and Holm-Hansen, O.: Effect of Fe on Productivity and Size Distribution of Antarctic Phytoplankton, Limnol. Oceanogr., 36, 1879–1885, 1991.

Hewes, C. D., Reiss, C. S., Kahru, M., Mitchell, B. G., and Holm-Hansen, O.: Control of phytoplankton biomass by dilution and mixed layer depth in the western Weddell-Scotia Confluence, Mar. Ecol.-Prog. Ser., 366, 15–29, 2008.

Hewes, C. D., Reiss, C. S., and Holm-Hansen, O.: A quantitative analysis of sources for summertime phytoplankton variability over 18 years in the South Shetland Islands (Antarctica) region, Deep-Sea Res. Pt. I, 56(8), 1230–1241, 2009.

Heywood, K. J., Naveira-Garabato, A. C., Stevens, D. P., and Muench, R. D.: On the fate of the Antarctic slope front and the origin of the Weddell Front, J. Geophys. Res., 109, C06021, doi:10.1029/2003JC002053, 2004.

Hofmann, E. E., Klinck, J. M., Lascara, C. M., and Smith, D. A.: Water mass distribution and circulation west of the Antarctic Peninsula and including Bransfield Strait, in: Foundations for Ecological Research West of the Antarctic Peninsula, edited by: Ross, R. M., Hofmann, E. E., and Quetin, L. B., American Geophysical Union, Washington, DC, 61–80, 1996.

Hofmann, E. E., Klinck, J. M., Locarnini, R. A., Fach, B., and Murphy, E.: Krill transport in the Scotia Sea and environs, Antarctic Science, 10, 406–415, 1998.

Holm-Hansen, O. and Riemann, B.: Chlorophyll a determination: Improvements in methodology, Oikos, 30, 438–447, 1978.

Holm-Hansen, O. and Mitchell, B. G.: Spatial and temporal distribution of phytoplankton and primary production in the western Bransfield Strait region, Deep-Sea Res., 38, 961–980, 1991.

Holm-Hansen, O., Kahru, M., Hewes, C. D., Kawaguchi, S., Kameda, T., Sushin, V. A., Krasovski, I., Priddle, J., Korb, R., Hewitt, R. P., and Mitchell, B. G.: Temporal and spa-

tial distribution of chlorophyll-*a* in surface waters of the Scotia Sea as determined by both shipboard measurements and satellite data, Deep-Sea Res. Pt. II, 51, 1323–1331, 2004.

Holm-Hansen, O., Kahru, M., and Hewes, C. D.: Deep chlorophyll-a maxima (DCMs) in pelagic Antarctic waters. II. Relation to bathymetric features and dissolved iron concentrations, Mar. Ecol.-Prog. Ser., 297, 71–81, 2005

Hopkinson, B. M., Mitchell, B. G., Reynolds, R. A., Wang, H., Selph, K. E., Measures, C. I., Hewes, C. D., Holm-Hansen, O., and Barbeau, K. A.: Iron limitation across chlorophyll gradients in the southern Drake Passage: phytoplankton responses to iron addition and photosynthetic indicators of iron stress, Limnol. Oceanogr., 52, 2540–2554, 2007.

Hoppema, M. H., de Baar, H. J. W., Fahrbach, E., and Hellmer, H. H.: Substantial advective iron loss diminishes phytoplankton production in the Antarctic Zone, Global Biogeochem. Cy., 17, 1025, doi:10.1029/2002GB001957, 2003.

Johnson, K. S., Gordon, R. M., and Coale, K. H.: What controls dissolved iron in the world ocean?, Mar. Chem., 57, 137–161, 1997.

Kahru, M., Mitchell, B. G., Gille, S. T., Hewes, C. D., and Holm-Hansen, O.: Eddies enhance biological production in the Weddell-Scotia Confluence of the Southern Ocean, Geophys. Res. Lett., 34, L14603, doi:10.1029/2007GL030430, 2007.

Koike, I., Holm-Hansen, O., and Biggs, D. C.: Inorganic nitrogen metabolism by Antarctic phytoplankton with special reference to ammonium cycling, Mar. Ecol. Prog. Ser., 30, 105–116,1986.

Korb, R. E., Whitehouse, M. J., Atkinson, A., and Thorpe, S. E.: Magnitude and maintenance of the phytoplankton bloom at South Georgia: a naturally iron replete environment, Mar. Ecol.-Prog. Ser., 368, 75–91, 2008.

Löscher, B. M., de Baar, H. J. W., de Jong, J. T. M., Veth, C., and Dehairs, F.: The distribution of Fe in the Antarctic Circumpolar Current, Deep-Sea Res. Pt. II, 44, 143–187, 1997.

Martin, J. H., Gordon, R. M., and Fitzwater, S. E.: Iron in Antarctic waters, Nature, 345, 156–158, 1990.

Öztürk, M.: Trends of trace metals (Mn, Fe, Co, Cu, Zn, Cd and Pb) distributions at the oxic-anoxic interface and in sulfidic water of Drammensfjord, Mar. Chem., 48, 329–342, 1995.

Öztürk, M., Steinnes, E., and Sakshaug, E.: Iron speciation in the Trondheim Fjord from the perspective of iron limitation for phytoplankton, Estuar. Coast. Shelf S., 55, 197–212, 2002.

Öztürk, M., Croot, P., Bertilsson, S., Abrahamsson, K., Karlson, B., Davis, R., Fransson, A., and Sakshaug, E.: Iron enrichment and photoreduction of iron under PAR and UV in the

presence of hydrocarboxylic acid: Implications for phytoplankton growth in the Southern Ocean, Deep-Sea Res. Pt. II, 51, 2841–2856, 2004.
Planquette, H. F., Statham, P., Fones, G.R., Charette, M. A., Moore, C. M., Salter, I., Nédélec, F. H., Taylor, S. L., French, M., Baker, A. R., Mahowald, N. and Jickells, T. D.: Dissolved iron in the vicinity of the Crozet Islands, Southern Ocean. Deep-Sea Research II, 54, 1999-2019, 2007.
Pollard, R., Treguer, P. and Read, J.: Quantifying nutrient supply to the Southern Ocean. Journ. Geophysical Res., 111, CO5011, doi:10.1029/2005JCO03076, 2006.
Pollard, R. T, Sanders, R., Lucas, M., and Statham, P.: The Crozet Natural Iron Bloom and Export Experiment (CROZEX), Deep-Sea Res. Pt. II, 45, 1905–1914, 2007.
Rönner, U., Sörensson, F., and Holm-Hansen, O.: Nitrogen assimilation by phytoplankton in the Scotia Sea, Polar Biol., 2, 137–147, 1983.
Sato, M., Takeda, S., and Furuya, K.: Iron regeneration and organic iron(III)-binding ligand production during *in situ* zooplankton grazing experiment, Mar. Chem., 106, 471–488, 2007.
Sañudo-Wilhelmy, S. A., Olsen, K. A., Scelfo, J. M., Foster T. D., and Flegal, A. R.: Trace metal distributions off the Antarctic Peninsula in the Weddell Sea, Mar. Chem., 77, 157–170, 2002.
Sullivan, C. W., Arrigo, K. R., McClain, C. R., Comiso, J. C., and Firestone, J.: Distributions of phytoplankton blooms in the Southern Ocean, Science, 262, 1832–1837, 1993.
Sunda, W. G. and Huntsman, S. A.: Iron uptake and growth limitation in oceanic and coastal phytoplankton, Mar. Chem., 50, 189–206, 1995.
Tovar-Sanchez, A., Duarte, C. M., Hernández-León, S., and Sañudo-Wilhelmy, S. A.: Krill as a central node for iron cycling in the Southern Ocean, Geophys. Res. Lett., 34, L11601, doi:10.1029/2006GL029096, 2007.
Twining, B. S., Baines, S. B., Fisher, N. S., and Landry, M. R.: Cellular iron contents of plankton during the Southern Ocean Iron Experiment (SOFeX), Deep-Sea Res., 51, 1827–1850, 2004.
Westerland, S. and Öhman, P.: Iron in the water column of the Weddell Sea, Mar. Chem., 35, 199–217, 1991.
Whitworth III, T., Nowlin Jr., W. D., Orsi, A. H., Locarnini, R. A., and Smith, S. G.: Weddell Sea Shelf Water in the Bransfield Strait and Weddell-Scotia Confluence, Deep-Sea Res., 41, 629–641, 1994.
Zhou, M., Niiler, P., Zhu, Y., and Dorland, R.: The Western Boundary Current in the Bransfield Strait, Antarctica, Deep-Sea Res. Pt. I, 53, 1244–1252, 2006.

Table 1. Accuracy and precision of the method by using the certified standard materials NASS-5 (National Research Council Canada) and spiked seawater samples. Method and resin blanks with procedural detection limits have been presented in the lower section of the table. The numbers in the parenthesis are the number of spikes and blanks.

		added (nM)	found (nM)	% recovery	% rsd
Open Ocean Seawater treated with Chelex-100* (22)	Spikes A	*		97.1	8.5
UVc+Chelex-100 treated seawater (3)*	Spikes B	2 nM	1.97±0.2	99	4.0
Coastal SW treated with Chelex-100 (4)*	Spikes C	20 nM	16.1±0.81	83	4.1
Coastal SW treated with Chelex-100-microwaved (5)*	Spikes D	20 nM	20.88±0.57	104	2.8
NASS 5 (3)	3.70 nM		3.10±0.33	84	7.2
NASS 5+microwaved (3)	3.70 nM		3.55±0.4	96	4.3
Chelex-100 Blank (8)			0.03±0.01 nmol		
Method blank (15)*∗			0.05±0.02 nmol		
Procedural detection limits (with pre-concentration factor 100)			0.03 nM		

* Seawater at pH 5.8 treated with Chelex-100 to remove all Chelex labile Fe. Spikes A include various added iron (0.5, 1, 1.5 and 18 nM), and spiked seawater were again Chelex-100 treated immediately after the addition of iron, Spikes C and D were treated with Chelex-100 24 h after addition, allowing the added iron to reach the equilibrium with existing natural organic ligands.
** Method blanks: 30 ml Milli-Q water+10 ml ammonium acetate solution treated exactly as sample with 0.5 g clean Chelex-100 and eluted similarly.

Table 2. Data for the 16 stations shown in Fig. 1b where concentrations of dissolved and total acid leachable Fe were determined. The five groupings of the stations are based on common characteristics, including water depth and proximity to different water masses such as Weddell Sea water and Drake Passage water. Depth of the upper mixed layer (UML) was calculated as the depth at which σ_θ differed by 0.05 from the mean density between 5 and 10 m depth. Values shown for temperature, salinity, and chl-*a* are mean values in the UML.

Group	Station No.	Station ID	Latitude, ° S	Longitude, ° W	Bottom Depth, m	UML Depth, m	Temp., °C	Salinity	Chl-*a*, mg m^{-3}
A	1	A0208	61.7	54.0	328	141	0.44	34.35	0.83
	2	A0410	62.2	55.0	540	44	−0.41	34.28	0.80
	3	A1214	63.2	59.0	147	112	0.35	34.39	1.18
	4	A1515	63.5	60.5	544	20	0.92	34.30	0.99
B	5	A0408	61.8	55.0	2012	45	1.85	34.25	1.13
	6	A0609	62.0	56.0	2150	39	2.16	34.27	1.40
	7	A0911	62.5	57.5	1485	27	2.92	34.29	1.88
C	8	Y2A1	62.3	61.5	1200	45	2.75	34.04	3.97
	9	Y8A1	62.1	61.1	1070	21	2.97	33.94	2.90
D	10	A2010	62.3	63.0	4078	14	3.46	33.64	1.04
	11	A1505	61.0	60.5	3708	20	3.62	33.80	0.10
	12	A0902	60.2	57.5	3284	19	3.57	33.80	0.14
	13	A0802	60.3	57.0	4079	41	3.66	33.83	0.69
E	14	A1412	62.7	60.0	913	24	2.28	33.97	3.66
	15	Y2A5	62.5	61.1	335	29	2.11	34.11	3.00
	16	Y5A5	62.4	60.9	90	30	1.77	34.15	2.10

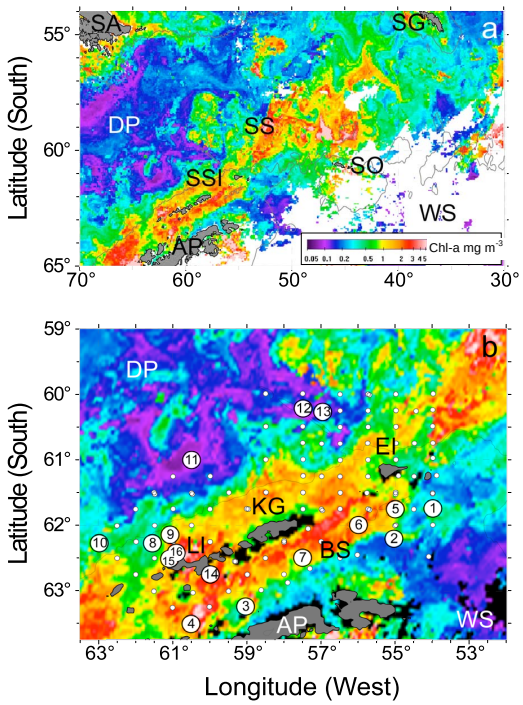

Fig. 1. Satellite images showing mean chlorophyll-*a* concentrations (mg m^{-3}) of surface waters in the Drake Passage-Scotia Sea regions of the Southern Ocean during January 2006. The color bar in the top image applies to both images. (**a**) Large scale map showing high chlorophyll-*a* concentrations in the central Scotia Sea downstream of the South Shetland Islands region. (**b**) Antarctic Peninsula region, with the numbered white circles showing location of stations where Fe concentrations were determined. Numbers refer to the stations listed in Table 2 that also provides hydrographic and biological data. The small white circles show the locations of all the stations in the AMLR sampling grid.The thin continuous line in (b) is the 1000 m depth isobath. AP, Antarctic Peninsula; DP, Drake Passage; EI, Elephant Island; KG, King George Island; LI, Livingston Island; SA, South America; SO, South Orkney Islands; SS, Scotia Sea; SG, South Georgia; SSI, South Shetland Islands; WS, Weddell Sea. White areas indicate no data due to cloud or ice conditions.

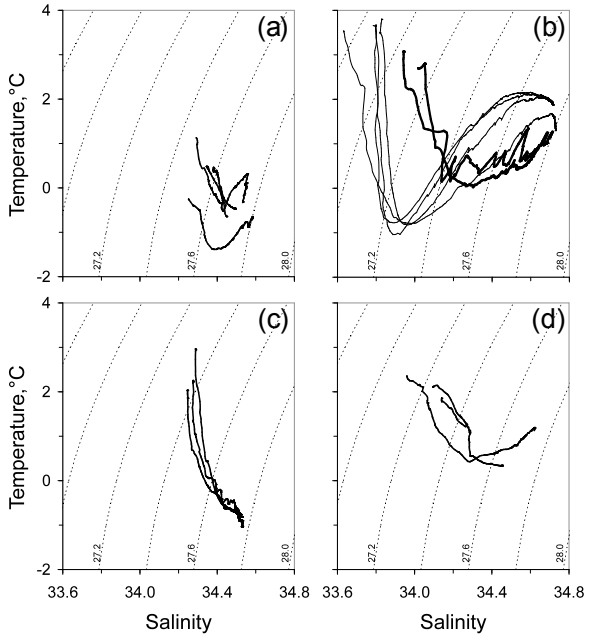

Fig. 2. Temperature/Salinity diagrams for the 16 stations where water samples were obtained for determination of Fe concentrations. Note that CTD profiles were obtained from the surface to 750 m, or to within ~10 m of the bottom at the shallower stations (bottom depths are given in Table 2). For station locations, see Fig. 1b. **(a)**, Group A stations (#1 to 4); **(b)**, Group D stations (#10–13) with light lines, and Group C Stations (#8–9) with dark lines; **(c)**, Group B stations (#5–7); **(d)**, Group E stations (#14–16). The thin dotted lines show isopycnal intervals (σ_θ) in temperature/salinity space.

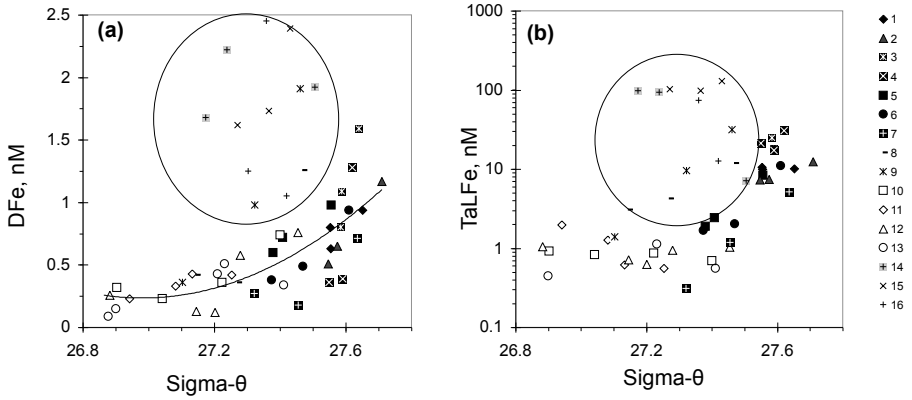

Fig. 3. Fe concentrations in relation to water density. (**a**) Dissolved Fe (DFe); (**b**) total acid leachable Fe (TaLFe). Open symbols are from Drake Passage waters. Closed symbols are from station close to or over the continental shelf. Note the change to a log scale ordinate for TaLFe. The stations within the circles are from the near-shore coastal survey (stations 8, 9, 15, 16) and station 14. Station numbers are shown in the column to the right.

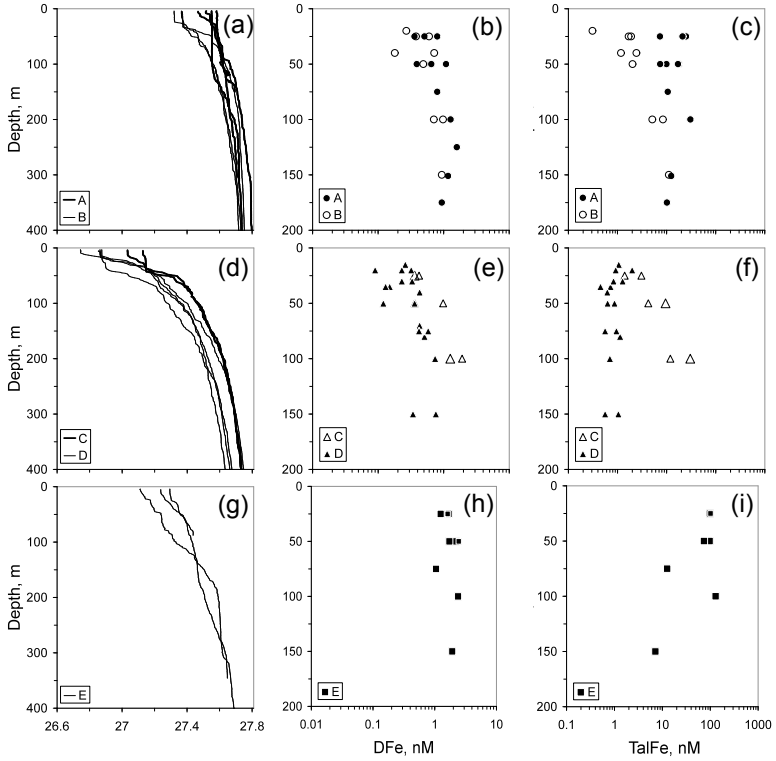

Fig. 4. Water density and Fe concentrations relative to water depth. Profiles show density (σ_θ; **a**, **d**, **g**), dissolved Fe concentrations (**b**, **e**, **h**), and total acid leachable Fe (**c**, **f**, **i**). Stations in groups A and B are shown in **a**–**c**; Stations in groups C and D are shown in **d**–**f**; Stations in groups E are shown in **g**–**i**. The stations within each of these five groups are listed in Table 2.

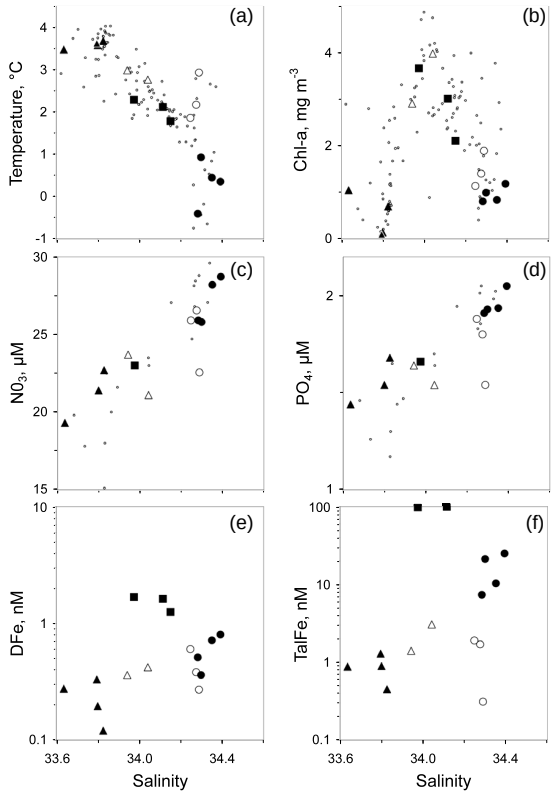

Fig. 5. Mean hydrographic, chemical, and biological values in the upper mixed layer in relation to salinity. **(a)** temperature; **(b)** Chl-*a*; **(c)**, nitrate; **(d)** phosphate; **(e)**, dissolved Fe; **(f)**, total acid leachable Fe. Group A stations (•), group B stations (o), group C stations (Δ), group D stations (▲), group E stations (■). The stations within each of these five groups are listed in Table 2. The small circles (dots) represent data from all the stations where Fe concentrations were not determined.

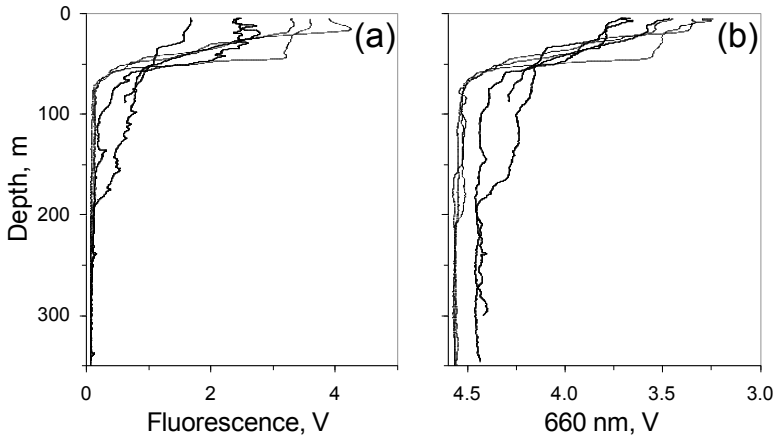

Fig. 6. Evidence of benthic input of Fe into coastal wasters. Upper water column characteristics at the three outer coastal survey stations (light lines, stationS #8 and 9, and one station in between) and at the three stations closest to shore (dark lines, stationS #15 and 16 and one station to the east of station #16). (**a**) profiles of in situ Chl-*a* fluorescence; (**b**) profiles of beam attenuation at 660 nm.

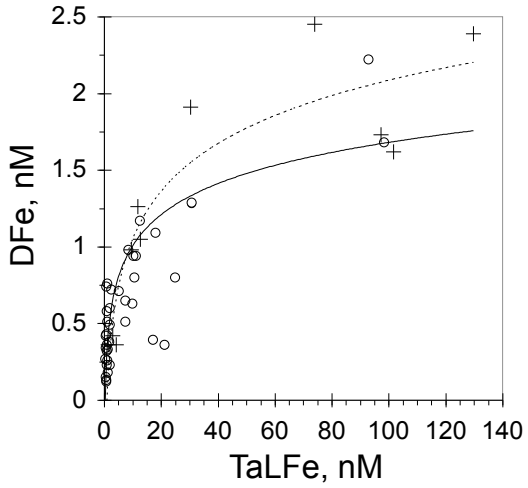

Fig. 7. Relation of dissolved Fe to total acid leachable Fe. The lower, dark regression line utilizes data from all stations. The upper, dashed regression line utilizes data from only the coastal survey stations (+, station #8–9, 15–16).

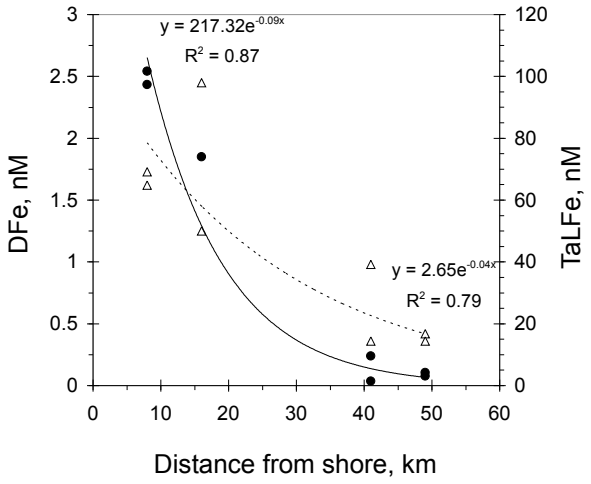

Fig. 8. Concentrations of Fe used to estimate scale lengths for dissolved and total acid leachable Fe. Exponential regressions were used to fit to data (curved lines) from four coastal stations (#8–9, 15–6) to determine the scale lengths for DFe (Δ, dashed line) and TaLFe (•, solid line). Equations for each regression are shown. Only surface values (<50 m) were used in these regressions.

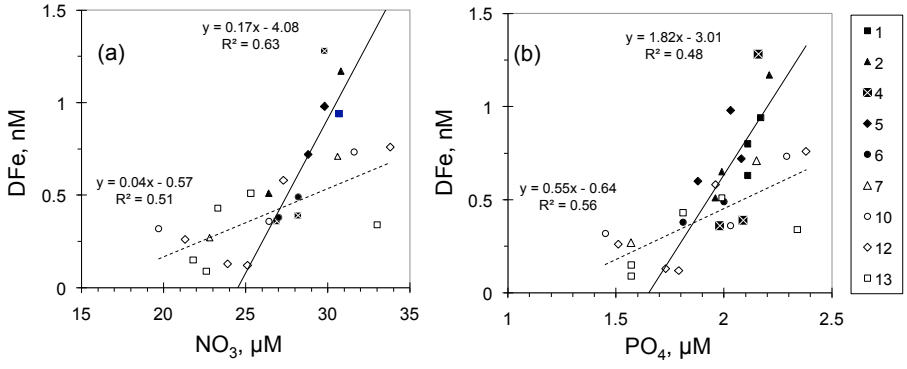

Fig. 9. Relationships between DFe and macronutrients at the nine stations where nutrient concentrations were determined. (**a**) DFe versus NO_3, (**b**) DFe vs. PO_4. Data from Drake Passage stations (#10, 12, 13) and station 7 are shown as open symbols and data from Bransfield Strait stations (#1–2, 4–6) are shown with closed symbols. Linear regressions, with equations, are shown for both zones. Station numbers are shown in the column to the right.

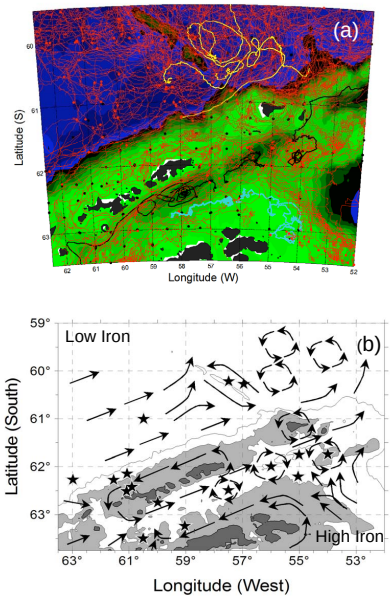

Fig. 10. Location of the 16 stations where Fe concentrations were determined in relation to water flow patterns in the Drake Passage-Antarctic Peninsula area. (**a**), Drifter tracks (in red, yellow, and black) showing the complexity of surface water flow. Green areas indicate increasing depth of the shelf regions, with the darkest green representing 2000 m depth. The small red and black circles indicate the location where each drifter was deployed. The drifter tracks in black illustrate the presence of eddies in Bransfield Strait. The drifter tracks in yellow show the effect of the Shackleton Transverse Ridge in steering water flow through the deep channel between the Ridge and Elephant Island, and the gyre-like tracks of the drifters to the east of the Ridge and north of Elephant Island. (**b**) Map of the sampling area showing generalized pattern of surface currents based on drifter track data, hydrographic data, and published water flow patterns. Figure has been modified from Fig. 1 in Hewes et al. (2009), but with more detail regarding water circulation. The darkest areas are islands and the northern tip of the Antarctic Peninsula. The lighter grey areas are bounded by the 500 m depth contour. The light continuous line is the 2000 m isobath. The topographical features (just to the west of stations 12 and 13) in the Drake Passage are part of the Shackleton Transverse Ridge, portions of which are <1000 m in depth. The stars show the locations of the 16 stations where Fe concentrations were determined. For identification of the land and sea areas refer to Fig. 1.